Knot localization in adsorbing polymer rings

B. Marcone,[1] E. Orlandini,[2,3] and A. L. Stella[2,3]
[1]*Dipartimento di Fisica, Università di Padova, I-35131 Padova, Italy*
[2]*Dipartimento di Fisica and Sezione CNR-INFM, Università di Padova, I-35131 Padova, Italy*
[3]*Sezione INFN, Università di Padova, I-35131 Padova, Italy*
(Received 5 September 2007; published 16 November 2007)

We study by Monte Carlo simulations a model of a knotted polymer ring adsorbing onto an impenetrable, attractive wall. The polymer is described by a self-avoiding polygon on the cubic lattice. We find that the adsorption transition temperature, the crossover exponent ϕ, and the metric exponent ν are the same as in the model where the topology of the ring is unrestricted. By measuring the average length of the knotted portion of the ring, we are able to show that adsorbed knots are localized. This knot localization transition is triggered by the adsorption transition but is accompanied by a less sharp variation of the exponent related to the degree of localization. Indeed, for a whole interval below the adsorption transition, one can not exclude a contiuous variation with temperature of this exponent. Deep into the adsorbed phase we are able to verify that knot localization is strong and well described in terms of the flat knot model.

DOI: 10.1103/PhysRevE.76.051804 PACS number(s): 36.20.Ey, 64.60.Ak, 87.15.Aa, 02.10.Kn

I. INTRODUCTION

Like other forms of topological entanglement of polymeric chains, knots have relevant consequences for both physics and biology [1]. It is known that they can be found in long closed macromolecules [2–5], such as circular DNA [6], and that they can affect important physical properties of them. For example, the migration velocity of circular DNA in gel electrophoresis depends on the knot type [7]. Among the various properties of knotted polymers, the determination of the *length* of the knots inside them, i.e., the length of the part of the chain which in some sense "contains" the entanglement responsible for the overall knottedness, has attracted much attention in recent years [8–12]. Indeed, the length of the knotted portion of the chain can be expected to play an important role in determining its physical properties. For example, the diffusion coefficient of knots tied into DNA by micromanipulation techniques should depend on the average size of the knots [13]. The action of topoisomerase on knotted DNA surely depends on how localized the knot is [14]. The folding dynamics of a knotted protein [15] should also depend on the size of the knot.

The determination, and even the definition, of the knot length, for real, three-dimensional (3D) polymers, is, however, quite difficult. Thus, historically, the problem was first faced for simplified models in which one imagines that a knotted polymer ring is confined in two dimensions. In this way the conformations of the ring reduce to those of a polymer network in 2D. The network is made only of loops and, under simplifying assumptions, maintains a fixed topology. These objects are called *flat knots* [16,17].

One possible physical realization of flat knots, which allows a link to be traced between them and "real" knots, is the following. Think of a knotted polymer in 3D, and imagine it is fully adsorbed on an attractive, flat surface; the polymer will then become two dimensional, and will consist of loops, since the original 3D chain was topologically a circle. The loops are made of segments joined at vertices, which in general correspond to overlaps of the adsorbed 3D polymer on itself. Usually, in the flat knot model the information on the sign of crossings is not taken into account. One can study the length of the "knot" inside this object, at least under some simplifying assumptions: namely, the number of crossings must be kept constant and at the minimum value compatible with the corresponding topology in 3D. In fact, in such a case the network will consist of a fixed number L of segments, while the knot length ℓ can be unambiguously put equal to the total length of the $L-1$ *smaller* ones. Now, one basic question about the knot length is whether knots are *localized* or not. Knots are said to be localized if, sending the polymer length N to infinity, their (average) length $\langle \ell \rangle$ does not grow as fast as N. This means that, in the *thermodynamic limit* ($N \to \infty$), the knot will behave as a pointlike object with respect to the whole polymer. More precisely, the localization can be of two types: strong and weak. It is said to be strong when $\langle \ell \rangle$ grows more slowly than any power of N {e.g., as $\log[\log(N)]$}, while it is *weak* if $\langle \ell \rangle \simeq N^t$, with the exponent t strictly less than 1 (but larger than 0). When a knot is delocalized, $\langle \ell \rangle$ grows as fast as N: in this case the knot will always occupy an extended part of the entire chain. From the point of view of statistical mechanics, the determination of the localization behavior of knots is a most interesting issue, since the exponent t is expected to be a *universal* (model-independent) quantity. Thus, it is not surprising that research on knot length has focused on this aspect; this is true for flat knots as well as for 3D knots, whose study inherited some terminology, and some ideas, of flat knot theory. For flat knots, Monte Carlo (MC) simulations, and theoretical calculations which employ the theory of polymer networks [18] allow one to make predictions on the value of t. It turns out that flat knots are strongly localized in the good solvent regime [17], but undergo a delocalization transition, and become delocalized, below the θ point [19,20].

The study of the localization behavior of 3D knots is more recent, and has been performed employing original strategies and computer simulations for a consistent statistical definition of knot length [9,10,12]. Indeed, the analytical treatment of the statistical mechanics of polymers constrained to have

the topology of a nontrivial knot is very hard [21]; this is mainly due to the *nonlocal* character of the knottedness constraint, which makes impossible its description by a *local* Hamiltonian, and thus prevents, e.g., the use of standard field-theoretical techniques. The Monte Carlo results obtained in [10,12] for $\langle \ell \rangle$ as a function of N have shown that prime knots in 3D are weakly localized, in the good solvent regime, with exponent $t \simeq 0.72$. The weak localization of 3D knots and the value of t determined in [10,12] for self-avoiding polygons (SAPs) on the cubic lattice have been subsequentially confirmed by simulations of off-lattice models [11].

Since flat knots should describe fully adsorbed knotted polymers, they are a useful model *per se*, and not only for the indirect, qualitative insights they provide into 3D knots. Adsorbed polymers are in fact extensively studied [22–24] and the adsorption transition is an important paradigm of polymer statistics [22].

For polymer rings adsorbed on a plane it is known that knotting can occur, and it has even been proven, for specific models, that it occurs with probability 1 for infinitely long chains [25,26]. Thus, the behavior of knots should be expected to play an important role in determining the physical properties of adsorbed polymers, as it does for swollen chains in 3D space. Flat knots represent only an extremely schematic model of adsorbed knotted polymers. In fact, a realistic model of an adsorbed polymer is given by a system consisting of a 3D polymer interacting with a short-range attractive, impenetrable, plane. It is known [27] that, in the case of unrestricted topology, this system exhibits a phase diagram with a desorbed phase at high temperature T and an adsorbed phase at low T; these two regimes are separated by a phase transition at a certain critical temperature T_c. At $T=0$ the polymer becomes a fully adsorbed 2D object, except possibly for *crossings* (which are always present if the topology of the polymer is different from that of an unknot). Thus, the ground state of real adsorbed knotted polymers should be described by flat knots; but for any nonzero T, adsorbed polymers have *excursions* (i.e., connected bunches of desorbed monomers) which can be quite extended, even if they have finite length on average.

So it is not clear if the true behaviour of real adsorbed knots for $T>0$ should be similar to that of polymer networks of fixed topology, or of their fully three-dimensional counterparts, or, maybe, of something in between. Recent measurements [28], on samples of knotted DNA adsorbed on a substrate, indicate that knots are rather localized. However, the chains in [28] seem not to behave as fully 2D objects. For example, the measured ν exponent is between the 2D and the 3D values. Thus, a full explanation of the behavior of these polymers may require one to go beyond the simple flat knot model. The model of adsorbed polymers we are going to study may be useful in this respect.

In this work we study the adsorption process of knotted ring polymers by means of Monte Carlo simulations. We focus on the adsorption transition and the low-temperature (adsorbed) regime, for the simplest prime knots (3_1, 4_1, 5_1, and 5_2). We check their thermodynamic properties, in order to trace any significant difference between the behavior of polymers with a fixed knot type and that of polymers with unrestricted topology. We estimate the temperature dependence of the average knot length $\langle \ell \rangle$ and search for a possible transition between the $T=\infty$ regime, where knots are expected to be weakly localized, and the fully adsorbed one ($T=0$), which corresponds to flat knots and thus to an expected strong localization.

The paper is organized as follows. In Sec. II we describe the model and the MC algorithms we use for the simulations. In Sec. III we present the numerical results and discuss the knot localization properties in different regimes. We close this section with a discussion on the relation between knotted polymers in the strongly adsorbed regime and the model of flat knots. Section IV contains our conclusions.

II. MODEL AND SIMULATION METHODS

A flexible polymer ring of N monomers close to an impenetrable surface can be modeled by an N-step self-avoiding polygon on the cubic lattice confined to the half space $z \geqslant 0$ and with at least one vertex anchored at the $z=0$ plane. To include a short-range attractive interaction between the surface and the polymer, an energy -1 is assigned to each vertex of the SAP having $z=0$ (visit). Denoting by $v(\omega)$ the number of visits of a given configuration ω the equilibrium properties of the model are described by the partition function

$$Z_N(T) = \sum_{\{\omega\}} e^{v(\omega)/\kappa_B T}. \tag{1}$$

where T is the absolute temperature and k_B is Boltzmann's constant. If the sum in Eq. (1) extends to configurations ω with all possile topologies, this model displays, in the thermodynamic limit, a second-order phase transition from a desorbed (high-T) phase to an adsorbed one (low T) [22,23]. In particular, there exists $T_c>0$ such that the limiting free energy

$$\mathcal{F}(T) = \lim_{N\to\infty} N^{-1} \log Z_N(T) \tag{2}$$

is equal to $-\log K_c^o$, independent of T, for all $T \geqslant T_c$ and is strictly greater than $-\log K_c^o$ for all $T<T_c$ [29]. The limiting value K_c^o denotes the critical fugacity of standard, noninteracting 3D SAPs [30], that is, the smallest value of the step fugacity K for which the generating function

$$G(T,K) = \sum_{N=1}^{\infty} Z_N(T) K^N \tag{3}$$

diverges. Let $\langle v \rangle$ be the average number of visits and

$$\rho(T) = \lim_{N\to\infty} \frac{\langle v \rangle}{N} \tag{4}$$

the limiting fraction of visits. Then for all $T>T_c$, $\rho(T)=0$ (desorbed phase), and for all $T<T_c$, $\rho(T)>0$ (adsorbed phase). Right at the transition temperature $T=T_c \approx 3.497$ [27] one expects

$$\rho(T_c) \sim N^{\phi-1}, \tag{5}$$

where ϕ is the crossover exponent which is believed to be very close to $1/2$ [27]. Another way to detect the adsorption

transition is by looking at the metric exponent ν that controls the scaling of the radius of gyration through the power law

$$\langle R_g \rangle \sim N^{\nu}. \tag{6}$$

Indeed, for $T \geqslant T_c$ one expects $\nu \approx 0.588$, i.e., the value for 3D SAPs [23], while for $T < T_c$ the value $\nu = 3/4$ of 2D SAPs [23] should be recovered.

The adsorption transition is one of the most succesfully studied transitions in the polymer literature [22,23], but if one restricts the sum of the partition function (1) to SAPs with a given knot type very few results are available so far. One of these is the rigorous, strict, bound

$$\mathcal{F}^{\emptyset}(T) < \mathcal{F}(T) \quad \forall \ T > 0, \tag{7}$$

where $\mathcal{F}^{\emptyset}(T)$ is the limiting free energy (1) restricted to the set of unknotted SAPs [25,26]. Inequality (7) implies that for every finite value of T the probability that the polygon is knotted goes to 1 as N goes to infinity [25,26]. The only exception would be the set of SAPs lying completely on the plane $z=0$ (2D SAPs), i.e., the zero-temperature limit for adsorbing rings. Of course, the knotting probability for finite N will depend on T and this has been investigated numerically [26]. No further studies have been performed so far on the effect of topological constraints on the adsorption transition but some reasonable assumptions can still be made. For example, one should expect that universal exponents such as the crossover exponent ϕ and the metric exponent ν do not depend on topological constraints. On the other hand, the critical temperature T_c could change when switching from the unrestricted to a restricted topology ensemble, but there is no strong theoretical insight into what should happen. Also, we cannot tell whether T_c should depend on the specific knot type or not. Given the difficulty in making any progress in this problem by analytical or rigorous means, a natural way to gain insight is by Monte Carlo simulations.

For a fixed temperature T, SAPs with a fixed knot type are generated by using a Monte Carlo approach based on the BFACF algorithm, [31]. This is an algorithm which samples along a Markov chain in the configuration space of polygons of variable N and with fixed knot type. The statistical ensemble considered is thus grand canonical, with a fugacity K assigned to each polygon step. We adopt this algorithm because it preserves the topology and is irreducible within each set of configurations having the same knot type [32]. At a given T we used a multiple Markov chain (MMC) procedure [33] in which configurations are exchanged among ensembles having different step fugacities [34]. This is done in order to improve the efficiency of the sampling, especially at low T where the SAPs are strongly adsorbed on the plane. The temperatures we considered are $T=3.50 \simeq T_c$ and $T=1.25$, 2.00, and 2.75, all much less than T_c. We also consider the value $1/T=0$ (noninteracting case) in order to compare it with the known situation of unweighted and geometrically unrestricted SAPs in 3D [10,12].

Despite the use of the MMC sampling technique, the BFACF algorithm becomes quite inefficient in the strongly adsorbed phase and for high values of N. To improve the sampling in this regime, we decided to use a hybrid scheme based on a combination of the BFACF with the pivot algorithm [35]. Since any pivot move can change the knot type of the resulting SAP [36], a check of its topology is needed before the move itself can be accepted. This is done by calculating the Alexander polynomial $\Delta(z)$ in $z=-1$ and $z=-2$ [37,38].

The BFACF algorithm does not preserve the value of N. Thus, in order to extract canonical averages at fixed N, we bin the data according to their N value. To collect enough statistics for a given N we used bins of width 10. In this respect the symbol $\langle \ _2 \rangle$ indicates for us averages taken within a bin centered in N and with size 10. The knot types considered in the simulations are the prime knots 3_1, 4_1, 5_1, and 5_2. However, most of the results we present here refer to the trefoil knot (3_1).

For each sampled SAP the length ℓ of the hosted knot τ is measured by determining the shortest possible arc that contains the knot. The procedure works as follows [10,12]. Given a knotted configuration, open arcs of different length are extracted by employing a recursive procedure. Each arc is then converted into a loop by joining its ends at infinity (i.e., at very far dinstance) with a suitable path. The presence of the original knot is finally checked by computing, on the resulting loop, the Alexander polynomial $\Delta(z)$ in $z=-1$ and $z=-2$ (see [12] for details). In all the simulations considered we sample, for each value of K, over 20 000 (independent) configurations. Since for fixed T a MMC scheme with ten different K values is used, the total number of configurations considered in the statistics of a given T amounts to 2×10^5.

III. RESULTS

A. Desorbed phase

To check the validity of our approach we first compare the known situation of 3D swollen SAPs [10,12] with the one of SAPs confined in the upper half space by an impenetrable nonattractive plane (noninteracting case). Since the constraint $z \geqslant 0$ should not play a significant role in knot localization, we expect strong similarities between the two cases. A first interesting issue concerns the value of K_c for the noninteracting and confined problem compared to the one (K_c^o) of the 3D case. For the whole class of SAPs (unrestricted topology) it is known that $K_c = K_c^o$ [29]. This result is obtained simply by translating each polygon in the bulk until the confining plane coincides with the bottom plane of the polygon. A similar argument can be used here for polygons with fixed knot type giving [up to the existence of $K_c(\tau)$] $K_c(\tau) = K_c^o(\tau)$ for all fixed knot types τ. This is indeed confirmed by our numerical results based on a MMC with ten different K's ranging from $K=0.2109$ up to 0.2130 [39] which give good evidence (within the confidence limit and for the prime knots considered) that $K_c(\tau) = K_c^o(\tau) = K_c^o$ [40]. We also confirm that at $T=\infty$ the metric exponent ν coincides (within error bars) in the two cases and that it is independent of the knot type (we estimate $\nu = 0.59 \pm 0.01$ for all knots considered). We now turn out attention to the behavior of the average knot length $\langle \ell \rangle$ as a function of N. Previous studies have shown that for 3D swollen knotted SAPs

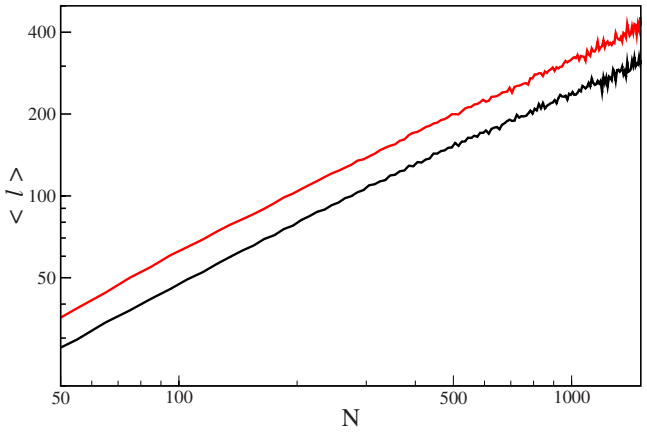

FIG. 1. (Color online) Average knot length $\langle \ell \rangle$ as a function of N for SAPs in the bulk (bottom curve) and for knotted SAPs confined in the $z \geqslant 0$ half space (top curve). In both cases the hosted knot is the trefoil knot (3_1). $\langle \ell \rangle \simeq N^t$ holds in both cases with $t = 0.73 \pm 0.03$. This value is consistent with that estimated for 3D SAPs in the bulk [10,12].

$$\langle \ell \rangle = AN^t + o(N^t), \tag{8}$$

with $t \approx 0.72$ for the trefoil [10,12]. Do we have the same behavior if the 3_1 SAPs are confined into one half space by an impenetrable (but still not attractive) plane? This seems to be the case as witnessed by Fig. 1 where a log-log plot of $\langle \ell \rangle$ as a function of N is reported for the two situations. The two curves look indeed linear and parallel to each other, confirming a weak localization regime with an exponent t that is the same (within error bars) in the two cases.

B. Adsorbed phase

When the attractive interaction between the SAP and the plane is switched on, the entropy is no longer the only ingredient in determining the equilibrium properties of the system. Instead, equilibrium is determined by the interplay between entropy and the energy gain in flattening the polymer on the plane. Moreover, when the topology of the ring is restricted to a fixed knot type, an additional entropic effect arises, because the entropies of rings with fixed topology and of rings with unrestricted topology are different.

From a numerical point of view, simulations of SAPs in the adsorbed regime require more effort than those for the desorbed one. Let $K_c(T|\tau)$ be the critical fugacity for adsorbing SAPs at temperature T and with knot type τ. For $T \geqslant T_c$ (desorbed regime), one can extend the argument given above for the nonadsorbing plane and show (up to the existence of the limiting free energy) that $K_c(T|\tau) = K_c(\tau) = K_c^o(\tau)$. On the other hand, for $T < T_c$ (adsorbed phase), $K_c(T|\tau)$ should decrease as the temperature decreases [41], and one cannot rely any more on a known value of K_c for simulations at a given T. Hence, for each value $T < T_c$ considered, the value of $K_c(T|\tau)$ must be estimated first (by short MC runs) before collecting a significant amount of data for that temperature.

Figure 2 shows the average knot size $\langle \ell \rangle$ as a function of N for SAPs with a trefoil knot tied in. Different curves correspond to different temperatures ranging from $T = 3.50$, a value just above the adsorption transition for the unrestricted case, down to $T = 1.25$, a value deep into the adsorbed phase. The plot in the noninteracting case is also reported for comparison. One can notice that the N behavior of $\langle \ell \rangle$ for SAPs close to the adsorption point $T = 3.5$ coincides with the one obtained for the noninteracting case. Since the adsorption point is the last point of the desorbed phase, this result shows that in this phase knots are weakly localized with an exponent t that does not depend on T, and coincides with the one found for 3D SAPs. Below the adsorption transition the situ-

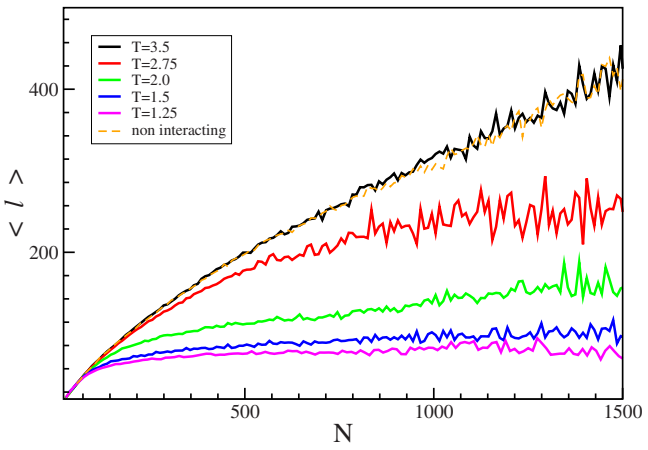

FIG. 2. (Color online) Average knot length $\langle \ell \rangle$ as a function of N for SAPs with knot 3_1. Different curves correspond to decreasing (from top to bottom) values of the temperature. The dashed curve corresponds to the noninteracting case. The corresponding values of t can be deduced from the values of c reported in Table II.

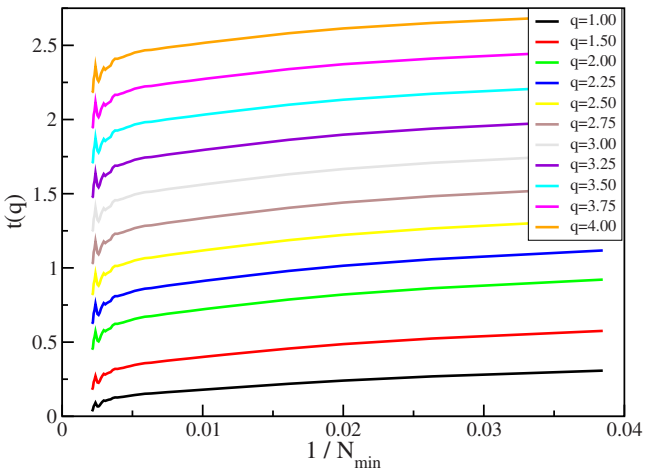

FIG. 3. (Color online) Finite-size scaling analysis of the exponents $t(q)$ for $T = 1.25$. For each value of q (q increases monotonically from bottom to top), $t(q)$ is obtained by fitting the data of $\langle \ell^q \rangle$ as a function of N with a power law in the range between N_{min} and $N_{max} = 1500$, with $N_{min} \ll N_{max}$. Here, different curves, corresponding to different values of q ranging from $q = 1.00$ (bottom curve) to $q = 4.00$ (top curve), are shown. To extract the asymptotic values we compute $t(q)$ as a function of N_{min} and extrapolate these values as $1/N_{min} \to 0$: This gives our best estimate of $t(q)$.

ation changes significantly: the average knot length still follows a power law behavior (8) with N, but the exponent t decreases as T decreases. More interestingly, if we go deeper into the adsorbed phase ($T=1.5, 1.25$) and look for sufficiently large N, $\langle \ell \rangle$ tends to a constant value. This is a signal of a strong localization regime ($t=0$), reminiscent of the one found for flat knots [17].

Clearly, if $t=0$, Eq. (8) does not give any insight into the degree of localization of knots. More detailed information can be obtained, however, by analyzing the N behavior of the probability distribution function (PDF) of the knot length, $P(\ell, N)$ [12]. In analogy with previous works on similar problems [12,42,43] one can assume the following scaling form:

$$P(\ell, N) = \ell^{-c} g(\ell / N^D), \tag{9}$$

where the scaling function g is expected to approach zero rapidly as soon as $\ell > N^D$, ($D \leqslant 1$). The quantity N^D is a cutoff on the maximum value ℓ can assume. We expect $D=1$, because there is no reason *a priori* to think that there exists some "topological cutoff" which limits the size of the knot. This is confirmed by our measurements, which yield $D \simeq 0.9-1$ at every T. Assuming g is integrable when its argument is sufficiently large, one can deduce that, for $0 < t \leqslant 1$, $c=2-t$, while $c>2$ always implies $t=0$. In this respect the desorbed phase (where $t \approx 0.75$) is characterized by $c=1.25$ [10], while at $T=0$ (fully adsorbed polymer) we could expect $c=2.69$, i.e., the value found for flat knots [17].

A common technique to analyze the scaling of the PDF (9) goes as follows. For a trial value of c and fixed N, one plots $P(\ell, N)\ell^c$ versus ℓ / N^D. Clearly, by varying N, different curves are displayed but if the values of c and D are close to the correct ones, all these curves should collapse onto a single one described by g. Eventually, after several trials, "optimal" values of c and D can be estimated. Unfortunately,

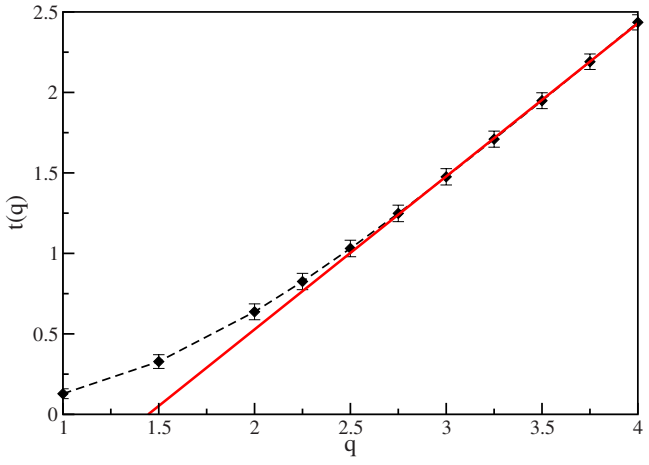

FIG. 4. (Color online) Analysis of the moments of the PDF $P(\ell, N)$ for $T=1.25$ and for the knot 3_1. The exponents $t(q)$, calculated as described in the caption of the previous figure and in the main text, are plotted against q. For $q \geqslant 2.5$ a good linear behavior is obtained and a linear fit in that range of q gives the estimate of c.

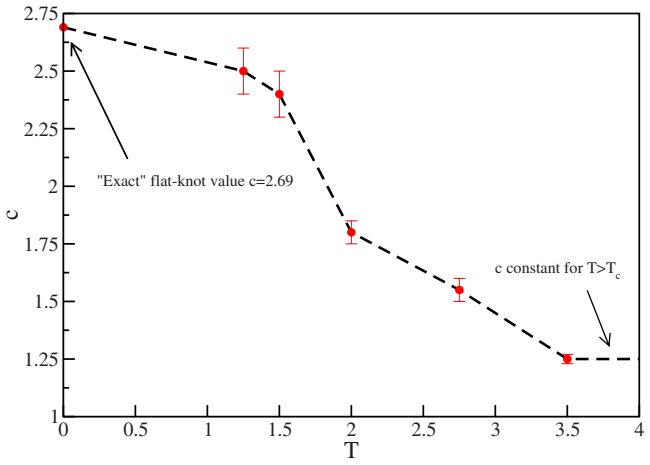

FIG. 5. (Color online) Estimated values of the exponent c for SAPs at the adsorption transition ($T=3.5$) and in the adsorbed phase ($T<3.5$). The knot considered is the trefoil. For $T \geqslant T_c$, we get $c=1.27 \pm 0.03$, independently of T (desorbed phase) This is consistent with $c=2-t$ and the expected value ($t \approx 0.75$) found in this regime.

to have a good matching of the curves, extremely good statistics are required, and this would not be feasible in this context.

We can instead perform an analysis based on the scaling behavior of the moments of the PDF in Eq. (1) [44]. This method relies on the following consideration: given the scaling behavior (9) for the PDF, its qth moment ($q>0$) should obey the asymptotic law

$$\langle \ell^q \rangle = \int \ell^{q-c} g(\ell / N^D) \sim N^{Dq+D(1-c)} \equiv N^{t(q)}, \tag{10}$$

and the two parameters D and c can be deduced by fitting the estimated exponents $t(q)$ against the order q [45] and performing a finite-size scaling analysis (see Fig. 3).

As shown in Fig. 4 for the $T=1.25$ case, the plots of $t(q)$ show deviations from linearity at relatively low q, due to finite-N scaling correction effects. This is typical for this kind of analysis [44]. However, for a sufficiently wide range of q, a linear behavior can be identified whose intercept gives an estimate of c.

Repeating the above procedure for the different temperatures considered one obtains the estimates plotted in Fig. 5 and reported in Table I.

TABLE I. Estimates of the exponent c for different values of T for trefoil knots. They have been obtained by the finite-size scaling analysis of the moments of the knot length as explained in the text.

T	c
3.50	1.27±0.03
2.75	1.55±0.05
2.00	1.80±0.05
1.50	2.42±0.10
1.25	2.55±0.10

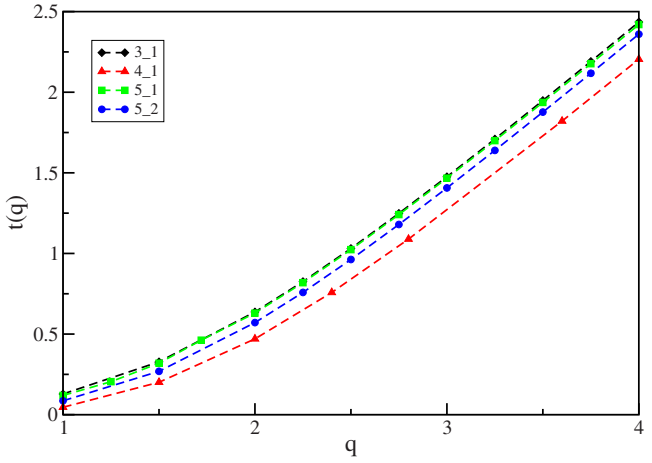

FIG. 6. (Color online) Estimates of the exponent $t(q)$ as a function of q for $T=1.25$ and for different prime knots. The error bars, that are not reported here for clarity, are of the same order as the ones reported for 3_1 in Fig. 4.

For $T \geqslant T_c$ the value of c is roughly 1.25 independent of T. This is consistent with the findings presented in the previous section. Indeed, in the desorbed regime (and up to the adsorption point included) the knot length exponent t is ≈ 0.72. As the temperature is lowered the polymer goes more deeply into the adsorbed phase and the c exponent increases, reaching, at $T=1.25$, the value $c=2.55\pm0.10$. The curve in Fig. 5 furnishes good evidence that knots in the adsorbed regime become strongly localized. The value of c at $T=1.25$ (2.55) agrees within the error bars with the value 2.69 found for flat knots, but it is possible that such value is reached precisely only in the $T \to 0$ limit.

One could take the intersection between the curve in Fig. 5 and the line $c=2$ as an estimate of a transition point T_{loc} between the weak and the strong localization regimes. This would suggest a localization transition occuring well below the adsorption transition. On the other hand, the curve in Fig. 5 is an estimate of $c(T)$ that relies on finite-N simulations and it is hard to decide whether $c(T)$ would show a sharp discontinuity as $N \to \infty$. Most intriguing would be the possibility of a range of temperatures in which the exponent c varies with T.

Results for other prime knots are quite similar to those presented for the trefoil knot. Figure 6 shows, for example, the estimates of $t(q)$ for 4_1, 5_1, and 5_2 deep in the adsorbed phase ($T=1.25$) compared with the one found for 3_1. All the curves look quite similar, and by performing a linear extrapolation we obtain the estimates of c given in Table II.

The estimated exponents are well compatible, within error bars, with each other

C. Equilibrium behavior of the knotted arc

Having established that the adsorption transition drives knots from being weakly localized to being strongly localized, it is now interesting to understand whether the knot behaves like the rest of the chain. In fact, one may wonder if the typical equilibrium configurations in the various phases

TABLE II. (Color online) Estimates of the exponent c for different prime knots at $T=1.25$.

Knot type	c
3_1	2.55 ± 0.10
4_1	2.60 ± 0.10
5_1	2.55 ± 0.10
5_2	2.56 ± 0.16

are the ones in which the knotted part is expelled out of the plane, so that the knot is free to fluctuate in the bulk. This can be checked by comparing, for example, the average height $\langle z \rangle$ of the whole SAP, $\langle z \rangle$, to the one restricted to its knotted part, $\langle z_{knot} \rangle$. Figure 7 shows the N dependence of $\langle z \rangle$, and $\langle z_{knot} \rangle$, at two values of the temperature. At $T=3.5$ (left panel) the two average heights are practically identical suggesting that, above the adsorption transition, the knotted part is indistinguishable from the hosting ring. This behavior seems to change at $T=1.25$ (deep adsorbed phase), where $\langle z \rangle$ is systematically lower than $\langle z_{knot} \rangle$. This could indicate that in the adsorbed regime the knotted part tends to be, on average, further away from the adsorbing plane than the whole chain. Note, however, that, even in the strongly adsorbed phase, the knotted part must keep a minimal number of excursions, in order to connect the minimal number of crossings required by its topology. It turns out that this minimal number of excursions is sufficient to explain the differences shown in Fig. 7 (right panel). This can be seen as follows. By simulationing unknotted rings at $T=1.25$ with $N \simeq 76$ monomers (which is roughly the equilibrium length of the 3_1 knot at that temperature), we observe that the average number of monomers in the excursions is $\langle b \rangle \approx 32$. On the other hand, the knotted portion of a knotted ring at the same temperature has $\langle b \rangle \approx 42$. In both cases, almost all excursions have height $z=1$. Hence the knot has, on average, ≈ 10 more monomers in the bulk with respect to tis unknotted counterpart. This is

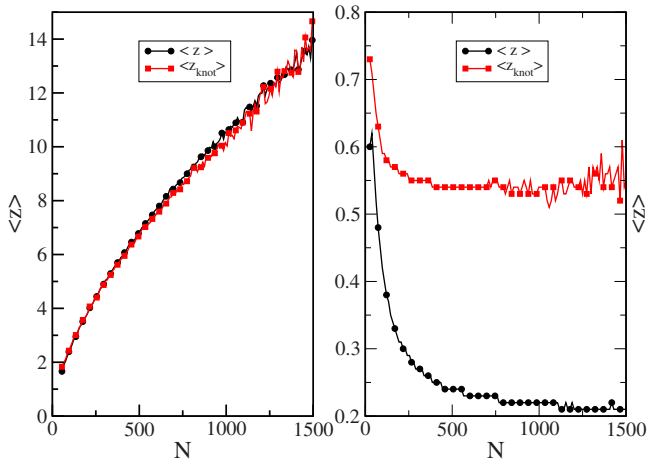

FIG. 7. (Color online) Average height $\langle z \rangle$ of the SAP and of its knotted counterpart ($\langle z_{knot} \rangle$) as a function of N. The left panel refers to $T=3.5$ (desorbed phase) while the right one to $T=1.25$ (strongly adsorbed phase).

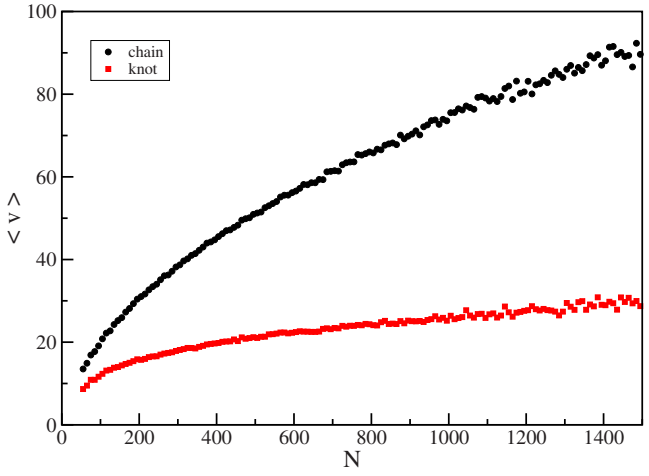

FIG. 8. (Color online) Average number of visits $\langle v \rangle$ of the whole SAP (top curve) and its knotted part (bottom curve) as a function of N. The temperature considered is $T=3.50 \simeq T_c$. The dashed line is still the one for the knotted one but now multiplied by $(N/\ell)^{\phi}$.

in agreement with the discrepancy observed in Fig. 7 (right panel). This difference is then due only to the unavoidable crossings pertaining to the knot. In fact each crossing requires at least three excursions of length 3 each, resulting in a minimal excursion length $3 \times 3 = 9 \simeq 10$ for the knotted part. Similar considerations apply to different knot types. This suggests that the knotted parts of a polymer are essentially no more desorbed than the rest of the chain.

Given that the position of the knot within the chain and with respect to the adsorbing plane has nothing special if compared to any remaining part of the chain, it is reasonable to expect that the equilibrium properties themselves, once restricted to the knotted part, will display the same features as those of the whole chain. To confirm this picture we estimate the average number of visits as a function of N for the knotted part and compare it with that of the whole polygon (Figs. 8 and 9). The temperature considered is the adsorption temperature T_c where the scaling behavior (5) with $\phi \approx 1/2$ is known to hold for *all* rings (unrestricted topology). By

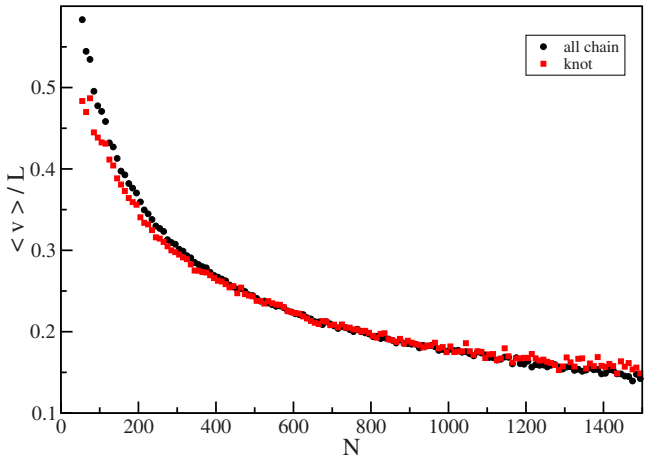

FIG. 9. (Color online) Average number of visits of Fig. 8 scaled by L where $L=N$ for the whole SAP and $N^{0.72}$ for the knotted part.

TABLE III. Estimates of the exponent ν for different values of T for trefoil knots. They have been obtained by a finite-size scaling analysis of Eqs. (6) and (12).

T	ν	ν_{knot}
∞	0.59±0.01	0.61±0.03
3.50	0.60±0.01	0.64±0.03
2.75	0.75±0.01	0.75±0.03
2.00	0.75±0.02	0.77±0.04
1.50	0.75±0.02	0.81±0.06
1.25	0.74±0.02	0.81±0.06

performing a simple power law fit we indeed get $\phi = (0.53 \pm 0.02)$ for the whole knotted SAP. Note that the estimate is for SAPs with *fixed knot type*, suggesting that the crossover exponent could be unaffected by topological constraints. To compute a crossover exponent restricted to the knotted part, the scaling 5 must be replaced by

$$\langle v_{knot} \rangle \sim \langle \ell \rangle^{\phi_{knot}}, \tag{11}$$

where $\langle v_{knot} \rangle$ indicates the number of visits of the knotted part of the ring. This gives $\phi_{knot} = (0.49 \pm 0.04)$, compatible with $\phi = \phi_{knot} = 1/2$.

Similarly one can define the metric exponent of the knotted portion of the chain, ν_{knot} as

$$\langle R_{knot} \rangle \sim \langle \ell \rangle^{\nu_{knot}}. \tag{12}$$

The estimates are reported in Table III and compared with those for the whole chain.

The ν_{knot} determinations are always slightly higher than those of ν and have slightly larger error bars. This is due to two effects: ℓ varies on a smaller range than N, and the data for R_{knot} are noisier too. The measured values of ν_{knot} are, however, comparable, within error bars, with the values of ν for the whole SAP. At *very* low T, when knots become strongly localized, the error bars on the estimates of ν_{knot} are quite big. This is mainly due to the relatively small values of $\langle \ell \rangle$ (between 16 and 100) which do not allow a good asymptotic analysis of (12).

D. Are adsorbed knots behaving as flat knots?

Our results show that the degree of localization of prime knots appear to be independent on the knot type (see Table II). This is consistent with the theory of flat knots which shows that, at leading order, all prime knots can be asymptotically described by the figure 8 graph reported in Fig. 10, whose behavior in the good solvent regime determines their strong localization [17]. However, adsorbed knots do not show the same degree of localization (measured by the exponent c presented above) as flat knots. In fact, they are always somehow less localized, i.e., they show values of c lower than that provided by flat knot theory. Note, however, that for $T=1.25$ the c values for adsorbed and flat knots are comparable within 2 standard deviations. On the other hand, since the Monte Carlo procedure deteriorates as T decreases, it would not be useful to try to go deeper in the adsorbed

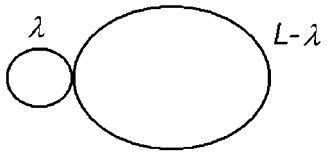

FIG. 10. Sketch of the figure 8 graph. Here L is the total length of the ring while λ is the length of the *shorter* loop, which can be identified with the knot length ℓ. It can be shown [17] that, when $L \gg \lambda$, the PDF for λ scales like λ^{-c_8}, with $c_8=2.69$.

phase. Indeed, at low T's, the estimates of c would be affected by error bars so large to make them not very significant.

We can then conclude that strongly adsorbed polymers should eventually behave as flat knots. If this happens at some T^* with $0<T^*<T_c$ or just in the limit $T\to 0$ it is, however, impossible to establish within our numerical precision.

Another distinction between adsorbed knotted rings and flat knots concerns the number of crossings $\mathcal{C}$, the chain makes with itself when it is *regularly* projected on the adsorbing plane [46]. Indeed, in the flat knot model the number of crossings is minimal (three for the 3_1, four for 4_1, etc.). This is crucial for the analytical treatment of the model and it would be interesting to see how close is the behavior of the strongly adsorbed rings to this assumption.

It turns out that while the average number of crossings $\langle \mathcal{C} \rangle$ of the whole chain increases (approximately linearly) with N, the same quantity restricted to the knotted portion is approximately constant and close to the minimum value allowed by the topology. For example, $\langle \mathcal{C}_{3_1} \rangle \approx 3.6$. The independence of N is quite reasonable since deep into the adsorbed phase knots are strongly localized. Moreover, strongly adsorbed rings tend to minimize their energy by maximizing the number of visits and, in the limit $T\to 0$, we should expect all the unimportant crossings to disappear leaving a 2D ring with just the essential (topological) crossings defining the knot [47].

At $T\neq 0$, however, fluctuations in the number of crossings are present and this could explain the deviation of the c exponent from the flat knot value for finite T values. In this respect, it could be useful to study the behavior of flat knots when the restriction on the minimal crossing number is relaxed. Recently, Guitter and Orlandini [16] introduced a model of flat knots on a lattice where the ring is a 2D polygon with a number of crossings which can be changed and tuned with an appropriate crossing fugacity. By implementing our knot detection technique on this model, we have estimated the average knot size for flat knots as a function of N for a wide range of values of the average crossing number. We find that flat knots are always strongly localized, independently of the average crossing number. This suggests that the crossing number is not a key feature to explain the value of c and that the flat knot model, even with a fluctuating number of crossings, is not a fair model for knotted rings in the adsorbed phase unless $T\to 0$.

IV. CONCLUSIONS

In this paper, we study by Monte Carlo simulations the equilibrium properties of self-avoiding polygons with fixed topology (knot) adsorbing onto an impenetrable wall. For unrestricted topology it is known that SAPs undergo an adsorption transition from a desorbed 3D swollen phase to an adsorbed phase. We first show that for SAPs with fixed topology the adsorption transition is still present. Moreover, we give numerical evidence that the metric exponent ν in the adsorbed and desorbed phases and the crossover exponent ϕ for SAPs with fixed topology, agree with the ones for the unrestricted topology case. Even nonuniversal quantities such as the critical adsorption temperature T_c and the critical fugacity K_c^o seem to be unaffected by the topological constraint.

By using an algorithm that allows the identification of the knotted portion of the SAP [10] we are able to focus on the equilibrium critical properties of this portion and compare them with those the whole SAP. We show that the knotted part behaves, in most respects, as any other connected subset of the ring with the same length. For example, we find that at $T=T_c$ the average energy of the knot scales as $\langle \ell \rangle^{\phi}$ where the value of ϕ agrees with that of the whole ring. The metric exponent of the knot ν_{knot}, which describes the scaling of the radius of gyration of the knotted part of the ring as a function of the knot length, is also consistent with the value of ν of the whole chain at every temperature. Furthermore, the average displacement of the knot from the plane (height) is the same of that of the whole ring, indicating that there is not a preferred height in space for the knotted portion.

The main emphasis of our work is, however, on the localization behavior of the knotted portion of the ring as T varies. We find that, for $T \geqslant T_c$, the average length $\langle \ell \rangle$ of the knotted portion grows as N^t where $t \approx 0.72$, consistent with the value found in [10,12] for knotted rings in the 3D bulk. This shows that knots in the desorbed phase and right at the adsorption transition are weakly localized, i.e., the presence of an attracting impenetrable plane does not change the localization properties of the knot. Below T_c, the knot becomes more and more localized, reaching a strong localization regime deep into the adsorbed phase. This crossover to more localized states is certainly triggered by the adsorption transition, but is quite smooth, as witnessed by the T dependence of the estimated localization exponent t. Thus, we can not exclude that below T_c there is a continuous variation of the exponent t with T. A possible alternative scenario is the existence of a sharp localization transition at some $T_{loc}<T_c$, such that t has the bulk value for $T>T_{loc}$, while $t=0$ (and $c=2.69$) below. To justify this latter scenario, one must assume that our data are affected by strong finite-size corrections, which cannot be numerically detected unless one performs simulations at much larger values of N. Note, however, that, even under this assumption, the possibility that $T_{loc}=T_c$ should be discarded on account of the observation that t starts to decrease only below T_c; a crossover region is expected to be more symmetric around the transition temperature T_{loc}. For sufficiently low values of T (deep in the adsorbed phase) the estimated c exponent agrees, within error bars, with the one found for flat knots. However, due to the large statistical uncertainty we cannot rule out the possibility that the flat knot regime is reached only in the limit $T\to 0$.

These results suggest that the relation between the flat knot model and adsorbed knots is nontrivial. The flat knot

regime is reached only at low enough T (or possibly at $T \to 0$) where the number of crossings, arising from a regular projection on the adsorbing plane, is close to the minimal value dictated by the topology. On the other hand, in the whole adsorbed phase many excursions in the bulk are allowed and give rise to a number of crossings that exceed the minimal one and that can fluctuate widely as N increases. These fluctuations are certainly responsible for the deviations from flat knot behavior observed at high enough T. The flat knot model is certainly not an adequate representation of knotted rings in the whole adsorbed phase.

ACKNOWLEDGMENTS

This work was supported by FIRB01 and MIUR-PRIN05.

[1] S. A. Wasserman and N. R. Cozzarelli, Science **232**, 951 (1989); D. W. Sumners, Not. Am. Math. Soc. **42**, 528 (1995).
[2] D. W. Sumners and S. G. Whittington, J. Phys. A **21**, 1689 (1988); N. Pippenger, Discrete Appl. Math. **25**, 273 (1989); E. J. Janse van Rensburg and S. G. Whittington, J. Phys. A **23**, 3573 (1990); M. C. Tesi, E. J. Janse van Rensburg, E. Orlandini, D. W. Sumners, and S. G. Whittington, Phys. Rev. E **49**, 868 (1994).
[3] M. Delbruck, *Mathematical Problems in the Biological Sciences*, Proceedings of the Symposium Applied on Mathematics Vol. 14 (American Mathematical Society, Providence, RI, 1962), p. 55.
[4] K. Koniaris and M. Muthukumar, Phys. Rev. Lett. **66**, 2211 (1991).
[5] E. Orlandini and S. G. Whittington, Rev. Mod. Phys. **79**, 611 (2007).
[6] V. V. Rybenkov, N. R. Cozzarelli, and A. V. Vologodskii, Proc. Natl. Acad. Sci. U.S.A. **90**, 5307 (1993).
[7] A. Stasiak, V. Katritch, J. Bednar, M. Michoud, and J. Dubochet, Nature (London) **384**, 122 (1996).
[8] V. Katritch, W. K. Olson, A. Vologodskii, J. Dubochet, and A. Stasiak, Phys. Rev. E **61**, 5545 (2000).
[9] O. Farago, Y. Kantor, and M. Kardar, Europhys. Lett. **60**, 53 (2002).
[10] B. Marcone, E. Orlandini, A. L. Stella, and F. Zonta, J. Phys. A **38**, L15 (2005).
[11] P. Virnau, Y. Kantor, and M. Kardar, J. Am. Chem. Soc. **217**, 15102 (2005).
[12] B. Marcone, E. Orlandini, A. L. Stella, and F. Zonta, Phys. Rev. E **75**, 041105 (2007).
[13] X. R. Bao, H. J. Lee, and S. R. Quake, Phys. Rev. Lett. **91**, 265506 (2003); A. V. Vologodskii, Biophys. J. **90**, 1594 (2006).
[14] B. Alberts, K. Roberts, D. Bray, J. Lewis, M. Ra, and J. D. Watson, *The Molecular Biology of the Cell* (Garland, New York, 1994).
[15] W. R. Taylor, Nature (London) **406**, 916 (2000); S. Wallina, K. B. Zeldovicha, and E. I. Shakhnovich, J. Mol. Biol. **368**, 884 (2007).
[16] E. Guitter and E. Orlandini, J. Phys. A **32**, 1359 (1999).
[17] R. Metzler, A. Hanke, P. G. Dommersnes, Y. Kantor, and M. Kardar, Phys. Rev. Lett. **88**, 188101 (2002).
[18] B. Duplantier, Phys. Rev. Lett. **57**, 941 (1986); B. Duplantier, J. Stat. Phys. **54**, 581 (1988).
[19] E. Orlandini, A. L. Stella, and C. Vanderzande, Phys. Rev. E **68**, 031804 (2003).
[20] A. Hanke, R. Metzler, P. G. Dommersnes, Y. Kantor, and M. Kardar, Eur. Phys. J. B **12**, 347 (2003).
[21] A. Yu. Grosberg and A. R. Khokhlov, *Statistical Mechanics of Macromolecules* (AIP Press, New York, 1994); A. L. Kholodenko and T. A. Vilgis, Phys. Rep. **298**, 251 (1998); T. A. Vilgis, *ibid.* **336**, 167 (1998).
[22] P. G. de Gennes, *Scaling Concepts in Polymer Physics* (Cornell University Press, Ithaca, NY, 1979).
[23] C. Vanderzande, *Lattice models of polymers* (Cambridge University Press, Cambridge, U.K., 1998).
[24] E. J. Janse van Rensburg, *The Statistical Mechanics of Interacting Walks, Polygons, Animals and Vesicles*, Oxford Lecture Series in Mathematics and its Applications Vol. 18 (Oxford University Press, New York, 2000).
[25] C. Vanderzande, J. Phys. A **28**, 3681 (1995).
[26] E. J. Janse van Rensburg, Contemp. Math. **304**, 137 (2002).
[27] R. Hegger and P. Grassberger, J. Phys. A **27**, 4069 (1994).
[28] E. Ercolini, F. Valle, J. Adamcik, G. Witz, R. Metzler, P. De Los Rios, J. Roca, and G. Dietler, Phys. Rev. Lett. **98**, 058102 (2007).
[29] J. M Hammersley, G. M. Torrie, and S. G. Whittington, J. Phys. A **15**, 539 (1982).
[30] Note that the critical value of $K_c = \exp(-\kappa)$ for 3D self-avoiding walks has been estimated to be 0.213 496 [see A. J. Guttmann, J. Phys. A **22**, 2807 (1989)].
[31] B. Berg, D. Foester, Phys. Lett. **106B**, 323 (1981); C. Aragão de Carvalho, S. Caracciolo, and J. Frohlich, Nucl. Phys. B **215**, 209 (1983); S. Caracciolo, A. Pellissetto, and A. D. Sokal, J. Stat. Phys. **60**, 1 (1990).
[32] E. J. Janse van Rensburg, and S. G. Whittington, J. Phys. A **24**, 5553 (1991); E. J. Janse van Rensburg, *ibid.* **25**, 1031 (1992).
[33] M. C. Tesi, E. J. Janse van Rensburg, E. Orlandini, and S. G. Whittington, J. Stat. Phys. **29**, 2451 (1996).
[34] E. Orlandini, *Numerical Methods for Polymeric Systems*, edited by S. Whittington IMA Volumes in Mathematics and Its Applications Vol. 102 (Springer, Berlin, 1998).
[35] S. Caracciolo, A. Pellissetto, and A. D. Sokal, J. Stat. Phys. **60**, 1 (1990).
[36] N. Madras and G. Slade, *The Self Avoiding Walk* (Birkhäuser, Boston, 1993); N. Madras, A. Orlitsky, and L. Shepp, J. Stat. Phys. **58**, 159 (1990).
[37] D. Rolfsen, *Knots and Links* (Publish or Perish, Berkely, CA, 1990).
[38] A. V. Vologodskii, A. V. Lukashin, M. D. Frank-Kamenetskii, and V. V. Anshelevich, Sov. Phys. JETP **66**, 2153 (1974).
[39] We recall that for adsorbing polymers $K_c = \exp(\kappa)$ for all $T > T_c$.

[40] The standard error of our determinations of $K_c(\tau)$ and $K_c^o(\tau)$ is of order 10^{-3}.
[41] This assumption is made by analogy with the known result for adsorbing SAPs with unrestricted topology [29].
[42] E. Carlon, E. Orlandini, and A. L. Stella, Phys. Rev. Lett. **88**, 198101 (2002).
[43] R. Zandi, Y. Kantor, and M. Kardhar, ARI: Bulletin of the Technical University of Istanbul **53**, 6 (2003).
[44] C. Tebaldi, M. De Menech, and A. L. Stella, Phys. Rev. Lett. **83**, 3952 (1999).
[45] Since for the distribution in Eq. (9) it is found in general that $t(q)=0$ for $q \leqslant q_c$ with $q_c>0$, the normalization constraint $\int p(\ell,N)=1$ does not imply $D(1-c)=0$, i.e., $c=1$.
[46] Note that a projection on the adsorbing plane ($z=0$) is not a regular one. We then project the SAP on a plane that makes a small angle with the $z=0$ plane.
[47] The reader should keep in mind that the polymer makes excursions outside the xy plane for every $T>0$.